J. Geogr. Sci. 2019, 29(2): 271-286
**DOI: https://doi.org/10.1007/s11442-019-1596-z**



# Quantitative attribution analysis of soil erosion in different geomorphological types in karst areas: Based on the geodetector method

WANG Huan[1,2], *GAO Jiangbo[1], HOU Wenjuan[1]

1. Key Laboratory of Land Surface Pattern and Simulation, Institute of Geographic Sciences and Natural Resources Research, CAS, Beijing 100101, China;
2. University of Chinese Academy of Sciences, Beijing 100049, China

**Abstract:** The formation mechanism and influencing factors identification of soil erosion are the core and frontier issues of current research. However, studies on the multi-factor synthesis are still relatively lacked. In this study, the simulation of soil erosion and its quantitative attribution analysis have been conducted in different geomorphological types in a typical karst basin based on the RUSLE model and the geodetector method. The influencing factors, such as land use type, slope, rainfall, elevation, lithology and vegetation cover, have been taken into consideration. Results show that the strength of association between the six influencing factors and soil erosion was notably different in diverse geomorphological types. Land use type and slope were the dominant factors of soil erosion in the Sancha River Basin, especially for land use type whose power of determinant (*q* value) for soil erosion was much higher than other factors. The *q* value of slope declined with the increase of relief in mountainous areas, namely it was ranked as follows: middle elevation hill> small relief mountain> middle relief mountain. Multi-factors interactions were proven to significantly strengthen soil erosion, particularly for the combination of land use type with slope, which can explain 70% of soil erosion distribution. It can be found that soil erosion in the same land use type with different slopes (such as dry land with slopes of 5° and above 25°) or in the diverse land use types with the same slope (such as dry land and forest with a slope of 5°), varied much. These indicate that prohibiting steep slope cultivation and Grain for Green Project are reasonable measures to control soil erosion in karst areas. Based on statistics of soil erosion difference between diverse stratifications of each influencing factor, results of risk detector suggest that the amount of stratification combinations with significant difference accounted for 55% at least in small relief mountain and middle relief mountainous areas. Therefore, the spatial heterogeneity of soil erosion and its influencing factors in different geomorphological types should be investigated to control karst soil loss more effectively.

**Keywords: soil erosion distribution; influencing factors; RUSLE model; geodetector; karst; Sancha River basin**

**Received:** 2018-08-19 **Accepted:** 2018-10-20

**Foundation:** National Basic Research Program of China, No.2015CB452702; National Natural Science Foundation of China, No.41671098, No.41530749

**Author:** Huan Wang (1993–), Master Candidate, specialized in the research of karst ecosystem services. E-mail: wangh.16s@igsnrr.ac.cn

***Corresponding author:** Gao Jiangbo, PhD, E-mail: gaojiangbo@igsnrr.ac.cn

## 1 Introduction

China is one of the countries with the most severe soil erosion problems in the world, with 37% of its land suffering from water and wind erosion (Li *et al*., 2008). In China, most severe water erosion occurs in its southwestern karst region, where soil erosion has become the leading factor hampering regional development (Dai *et al*., 2018). The unique dual aboveground/belowground hydrological structure (Yan *et al*., 2018), a humid climate and a carbonate basement are the internal causes for soil erosion in China's karst region, and poorly managed human activity is the external driving force. Land reclamation from forests, grassland destruction and slope cultivation exacerbate soil erosion, and topsoil loss leads to more serious rocky desertification problems (Wang *et al*., 2004; Zhang *et al*., 2013b; Hou *et al*., 2016), which in turn result in land degradation, frequent droughts and floods and near ecosystem collapse (Gutierrez *et al*., 2014; Peng *et al*., 2018). A scientific understanding and quantitative assessment of the effects of geographic environmental factors, human activity and their combination on soil erosion is of vital importance for curbing soil erosion and advancing the restoration of ecosystems that have suffered from rocky desertification in China's karst region.

Researchers in China and elsewhere have attached great importance to the high ecosystem vulnerability, unique hydrogeologic structure and rocky desertification problems in China's karst region and have conducted a number of studies focusing on soil erosion in this region. Wang *et al*. (2013), for purposes of identifying the driving factors of karst soil erosion, examined the relationships between land use and vegetation coverage and soil erosion in the Wujiang River Basin in Guizhou. They noted that dry land suffered from the most severe soil erosion and that converting slope farmland to terraced farmland could effectively prevent soil erosion (Xu and Shao, 2006). Zhang *et al*. (2007) noted that vegetation destruction and land reclamation and cultivation tended to aggravate subsurface soil leakage loss from slopes underlain primarily by carbonate rocks. Xiong *et al*. (2012) concluded that the local geology and geomorphology are the factors controlling the conservation and development of vulnerable ecosystems that have suffered from rocky desertification and determine the structure and operational pattern of karst ecosystems. In a quantitative study for estimating the amount of soil erosion, Bai *et al*. (2013) used cesium-137 ($^{137}$Cs) and excess lead-210 ($^{210}Pb_{ex}$) to analyze the response of soil erosion to land-use changes in a karst basin and found that net soil erosion rates increased significantly after 1979 when deforestation occurred. Feng *et al*. (2016) simulated soil erosion in karst basins in Guangxi using the revised universal soil loss equation (RUSLE) model and the $^{137}$Cs tracing method. When considering changes in both land use and precipitation, they found relatively good agreement between the results obtained using the two methods. However, due to the discontinuous nature of surface runoff in the karst areas, they found that determining the slope length ($L$) factor in the RUSLE model requires a high resolution digital elevation model (DEM). Based on a slope runoff plot experiment, Peng and Wang (2012) found that different precipitation mechanisms and land-use patterns affected soil erosion and surface runoff considerably differently.

Although these studies focused on the effects of geographic environmental factors and human activity on soil erosion, there is still a lack of studies that comprehensively compare factors and combinations of variables. In addition, most studies used correlation or regression analysis and focused little on quantitative analysis of multi-factors and their interactions.

In fact, conventional statistical or spatial analyses are poorly suited for quantifying the factors affecting soil erosion. In comparison, the geodetector method can reveal the driving force behind a geographic phenomenon by detecting its spatial stratified heterogeneity. This method has been extensively used in the social sciences (Zhan *et al*., 2015; Li *et al*., 2017) and human health research (Hu *et al*., 2011) and is being popularized in natural (Luo *et al*., 2016) and environmental (Tong *et al*., 2014) sciences. Its core assumption is that if a certain independent variable has a significant impact on a certain dependable variable, then there is relatively good agreement between the spatial distribution patterns of the independent and dependent variables (Wang and Xu, 2017). Therefore, in this study, we conducted a multi-factor attribution analysis of soil erosion in a karst basin using the geodetector method, with the spatial distribution of geomorphological types as the macroscopic background. The goal was to distinguish the dominant factors affecting soil erosion in areas of various geomorphological types and their interactions and thus provide a scientific basis for formulating ecological controls and environmental protection policies in karst regions.

## 2 Data and methods

### 2.1 Study area

The Sancha River Basin, a typical karst peak cluster-depression basin in northwestern Guizhou province, was selected as the study area. Situated in the southwestern Wujiang River Basin in Guizhou (Figure 1), the Sancha River Basin encompasses an area of 4,860 km$^2$. The Sancha River, 325.6 km in length, is a primary tributary of the Wujiang River. The bedrock underlying the study area consists mainly of carbonate rocks and a small amount of insoluble rocks. Due to the dual aboveground/belowground structure formed by karstification, an aboveground river network is absent, however there is a well-developed

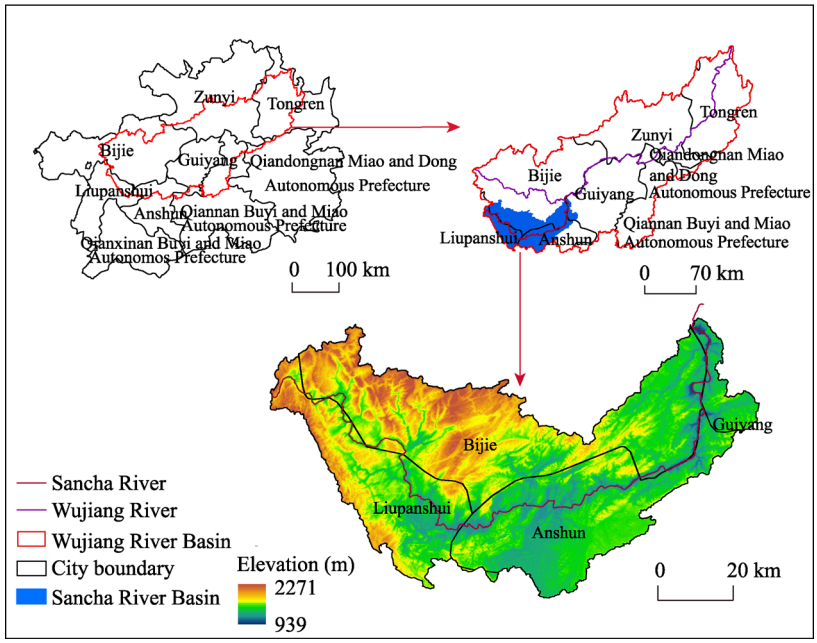


**Figure 1** Location of the Sancha River Basin, Guizhou province, China

belowground river network in the Sancha River Basin. Most of the karst landform develops vertically, resulting in large areas of steep slopes (Cai *et al*., 2015) and favorable conditions for soil erosion. The soil layers in the study area are thin with slow formation process, poor ecologic and physical properties, and a lack of layer of semi-weathered parent material. Adhesion between the soils and rocks is relatively weak, and there is a distinct soft/hard interface between the soils and rocks. As a result, the study area is prone to soil erosion and sliding of soil blocks (Cai *et al*., 2015). The Sancha River Basin has a subtropical monsoon climate with abundant precipitation (annual average of approx. 1100 mm), most of which falls between May and October and rainstorm is common. The study area lacks a variety of plant communities, and the forests perform relatively weakly in terms of ecologic functions. The local karst topography has a fragmented surface with scattered farmland on it and is densely populated. Man–land conflicts are thus prominent in karst areas. Poorly managed local land-use patterns have resulted in severe soil erosion.

### 2.2 Data sources and processing

The data required for soil erosion calculation based on the RUSLE model include: high resolution (9 m) DEM data (Google Earth) due to the sensibility of topographic factor to the resolution of DEM data; two Landsat-8 images (30 m) in 2010 (https://glovis.usgs.gov) were used to interpret land use data based on field fixed collecting points (Figure 2c) and with supervision classification method under ENVI software, and the Kappa coefficient was 0.81. Soil data with physical properties (1-km resolution) was acquired from the Harmonized World Database version 1.1 established by the Food and Agriculture Organization of the United Nations and the International Institute for Applied System Analysis; precipitation data of 28 meteorological stations in the Sancha River Basin and its surrounding areas in 2010 (National Meteorological Information Center, http://data.cma.cn) were interpolated to obtain the raster date using the ANUSPLIN software (Hutchinson, 2002); according to the research of Zhou *et al*. (2009), there are five geomorphological types in the study area (Figure 2a), including small relief mountain, middle relief mountain, middle elevation plain, middle elevation hill and middle elevation terrace, the data were collected from Data Center for Resources and Environmental Sciences, Chinese Academy of Sciences (http://www.resdc.cn). Quantitative attribution analysis of soil erosion of the five different geomorphological types have been done to detect the dominant factors, the following factors were used in this study: lithology (http://www.resdc.cn) (Figure 2b), land use type (Figure 2c), slope (Figure 2d), rainfall (Figure 2e), vegetation coverage (250-m, https://glovis.usgs.gov) (Figure 2f), and elevation (Figure 1).

### 2.3 Methods

#### 2.3.1 RUSLE model

Under the background of land degradation and serious soil erosion, traditional soil erosion research method, such as runoff plot method and artificial rainfall experiment, cannot obtain soil erosion data timely at a basin scale. Relying on basic research for ecological management could lead to the lag of soil and water conservation measures (Zeng *et al*., 2017), thus model simulation methods are gradually favored. Among them, the RUSLE model (Renard *et al*., 1997) is one of the most popular models in the world, which not only makes up for the

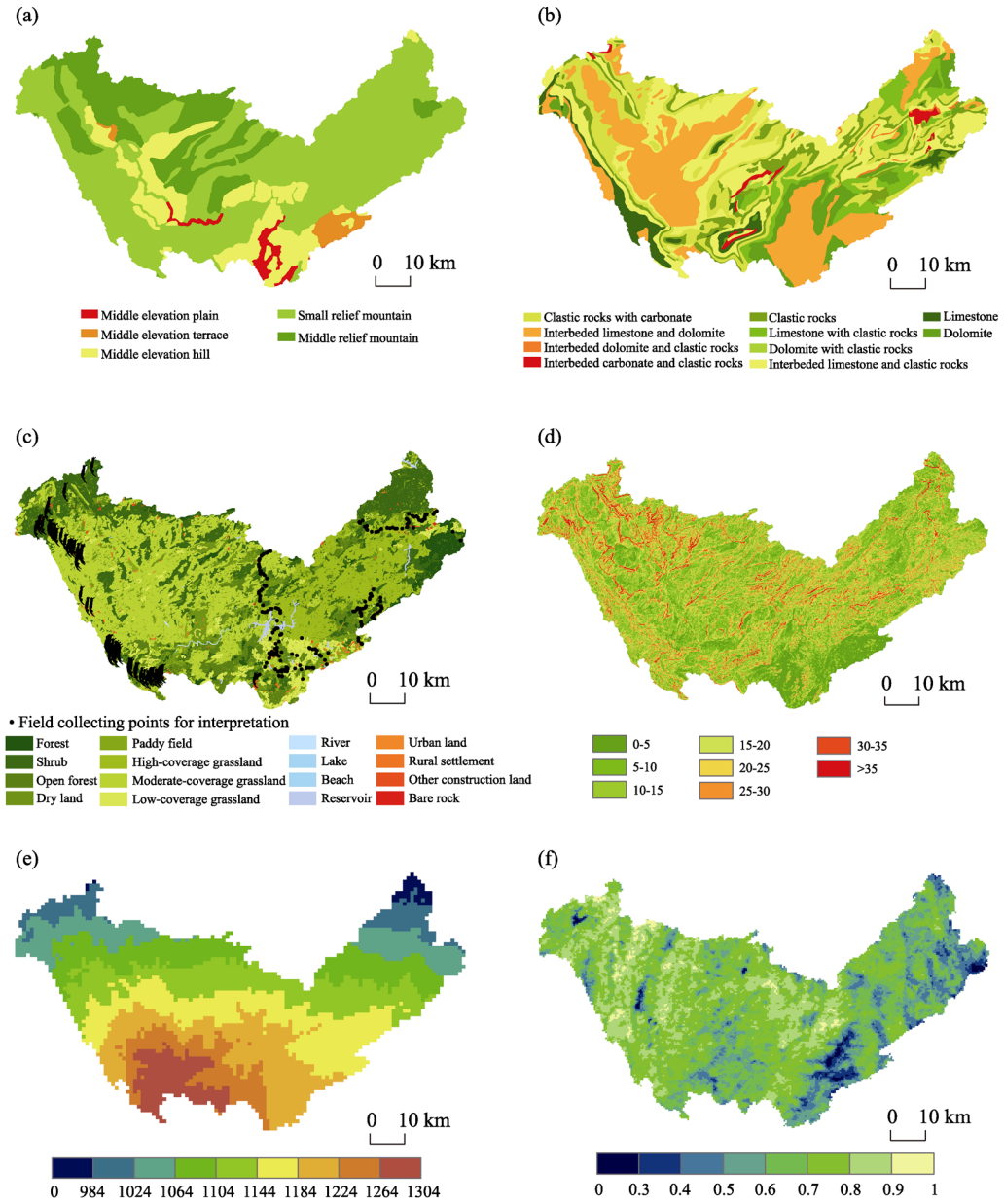


**Figure 2** Geomorphological types in the Sancha River Basin (a) and influencing factors of soil erosion (b. lithology; c. land use type; d. slope; e. rainfall; f. vegetation coverage)

limitations of field observations in large-scale applications, but also is suitable for multi-scale simulation studies (Wang *et al.*, 2013; Feng *et al.*, 2016). Satisfying results of different scale simulations have been obtained. The mathematical expression is as follows:

$$A = R \times K \times LS \times C \times P \quad (1)$$

where $A$ is annual soil erosion rate (t ha$^{-1}$a$^{-1}$), $R$ is rainfall erosivity factor (MJ mm ha$^{-1}$h$^{-1}$a$^{-1}$), $K$ is erodibility factor (t ha h MJ$^{-1}$mm$^{-1}$ha$^{-1}$), $LS$ is topographic factor, $C$ is vegetation cover and management factor, and $P$ is the conservation and supporting factor.

The $R$ factor reflects the effect of rainfall characteristics impacting on soil erosion, such as rainfall intensity and amount. The equation proposed by Wischmeier and modified by

Arnoldus (1980) was used in this study to simulate rainfall erosivity factor. The equation is as follows:

$$R = \sum_{i=1}^{12} \left( 1.735 \times 10^{1.5 \times \log \frac{pi^2}{p} - 0.8188} \right) \tag{2}$$

where $pi$ and $p$ represent monthly mean and annual mean rainfall, respectively, $i$=1,2,…, 12, representing month.

$K$ is erodibility factor, a function of soil properties. The method of the erosion-productivity impact calculator (EPIC) proposed by Williams *et al*. (1989) was used to calculate the $K$ factor in this study:

$$K = \left\{ 0.2 + 0.3e^{\left[ -0.0256 W_d \left( 1 - W_i / 100 \right) \right]} \right\} \times \left( \frac{W_i}{W_i + W_t} \right)^{0.3} \times \left[ 1 - \frac{0.25 W_c}{W_c + e^{(3.72 - 2.95 W_c)}} \right] \times \left[ 1 - \frac{0.7 W_n}{W_n + e^{(-5.51 + 22.9 W_n)}} \right] \tag{3}$$

$$W_n = 1 - \frac{W_d}{100} \tag{4}$$

where $W_d$ is sand fraction (%), $W_i$ is silt fraction (%), $W_t$ is clay fraction (%), and $W_c$ is content of soil organic carbon (%).

Due to the dual hydrological structure, the $LS$ factor was sensitive to the RUSLE model, high resolution DEM data were used in this study. The $S$ factor was calculated based on the equation proposed by McCool *et al*. (1987). The $L$ factor was computed with the equation which was first proposed by McCool *et al*. (1989) and modified by Zhang *et al*. (2013a). The equations are as follows:

$$S = 10.8 \times \sin\theta + 0.03 \quad (\theta < 9\%,\ \lambda > 4.6\ \text{m}) \tag{5}$$

$$S = 16.8 \times \sin\theta - 0.50 \quad (\theta \geqslant 9\%,\ \lambda > 4.6\ \text{m}) \tag{6}$$

$$S = 3.0 \times (\sin\theta)^{0.8} + 0.56 \quad (\lambda \leq 4.6\ \text{m}) \tag{7}$$

$$L = \left( \frac{\lambda}{22.13} \right)^{\alpha} \tag{8}$$

$$\alpha = \left( \frac{\beta}{\beta + 1} \right) \tag{9}$$

$$\beta = \frac{\sin\theta}{3 \times (\sin\theta)^{0.8} + 0.56} \tag{10}$$

where $\theta$ is slope, $\lambda$ is slope length, $\alpha$ is variable length-slope exponent, and $\beta$ is a factor relative to slope gradient.

The calculation of $C$ and $P$ factors has not formed a unified standard. Previous research (Xu and Shao, 2006; Feng *et al*., 2016) in karst areas has been referred in this study (Table 1).

The factors in the RUSLE model differed in terms of data source and resolution. Therefore, data normalization was needed. In ArcGIS 10.2, the spatial resolution and projected coordinates of the factors in the RUSLE model were normalized to 30 m and to the Albers_conic equal-area projection, respectively. The spatial resolution of the land-use data

**Table 1** *C* and *P* value

| Land use type | Paddy field | Dry land | Forest | Open forest | Shrub | Grassland | Water | Construction land | Bare rock |
|---|---|---|---|---|---|---|---|---|---|
| *C* value | 0.1 | 0.22 | 0.006 | 0.01 | 0.01 | 0.04 | 0 | 0 | 0 |
| *P* value | 0.15 | 0.4 | 1 | 1 | 1 | 1 | 0 | 0 | 0 |

used in this study was 30 m, which was used as a reference resolution. The 9-m slope length and steepness (*LS*) factor was upscaled to 30 m. Because the local precipitation varies insignificantly within a range of 1 km, particularly on annual and monthly scales, downscaling the interpolated 1-km precipitation data to 30 m was appropriate. Since the soil types varied a little within a range of 1 km and the value of soil erodibility (*K*) factor was relatively low, we downscaled the soil type data to 30 m, which did not affect the accuracy.

### 2.3.2 Geodetector method

The geodetector is a method to reveal the driving force of an event by detecting the spatial stratified heterogeneity of the variables which means that the sum of the variance in each layer is smaller than the total variance of the whole region, the heterogeneity was measured by the *q* value (Wang and Xu, 2017). The method is mainly applied to the identification and mechanism of the influencing factors of spatial heterogeneity (Li *et al*., 2017). The influencing factor needs to be categorical variables, which was important for the detection of influencing factors for soil erosion. The geodetector contains four modules: factor detector, risk detector, interaction detector and ecological detector.

Factor detector detects the spatial heterogeneity of dependent variable and the power of determinant of the independent variables on the dependent variable, the value is measured by the *q* value (Wang *et al*., 2010).

$$q = 1 - \frac{\sum_{h=1}^{L} N_h \sigma_h^{\,2}}{N\sigma^2} = 1 - \frac{SSW}{SST} \tag{11}$$

$$SSW = \sum_{h=1}^{L} N_h \sigma_h^{\,2} \quad SST = N\sigma^2 \tag{12}$$

where $h$=1, ..., $L$ is the layer of independent variable $X$, $N_h$ and $N$ are the number of sample units in layer $h$ and the total region, respectively. $\sigma_h^{\,2}$ and $\sigma^2$ are the variance in the $h$ layer and the variance in the region. *SSW* means the sum of spatial variance of each layer, *SST* means total variance of $Y$ in the region, $L$ means the layer number of factor $X$. The $q$ value lies in [0, 1]. If factor $X$ completely controls the soil erosion, the $q$ value equals to 1; if the factor $X$ is completely unrelated to $Y$, the $q$ value equals to 0.

Ecological detector compares whether the influence of factors impacting on soil erosion is significantly different or not by using the *F*-test (Wang and Xu, 2017); the interaction detector is the preponderance of geodetector method compared to other statistical methods, which can identify the interacting form by comparing the $q$ values of single factor and the interaction $q$ values. The assumption for interaction detector was different from the traditional statistical methods, such as the multiplication of logistic regression hypotheses, but as long as interaction exists, it can be detected, the interaction types can be seen in Table 2; the risk detector can determine whether there is a significant difference in soil erosion between the layers of the impact factor and identify the areas of high risk of soil erosion.

**Table 2** Types of interaction between two covariates

| Description | Interaction |
|---|---|
| $q(X1 \cap X2) < Min(q(X1), q(X2))$ | Weakened, nonlinear |
| $Min(q(X1), q(X2)) < q(X1 \cap X2) < Max(q(X1), q(X2))$ | Weakened, single factor nonlinear |
| $q(X1 \cap X2) > Max(q(X1), q(X2))$ | Enhanced, double factors |
| $q(X1 \cap X2) = q(X1) + q(X2)$ | Independent |
| $q(X1 \cap X2) > q(X1) + q(X2)$ | Enhanced, nonlinear |

The input variables for the geodetector model needed to be converted to categorical variable. Thus, continuous variables needed to be discretized. The land use type, lithological type and geomorphological data were classified according to their original categories. Based on the data discretization method proposed by Wang and Xu (2017) and priori knowledge, the vegetation coverage was assigned to eight ranges: <0.3, 0.3–0.4, 0.4–0.5, 0.5–0.6, 0.6–0.7, 0.7–0.8, 0.8–0.9, and 0.9–1. Precipitation and elevation data were divided into nine equal intervals. Slope gradients were assigned to eight categories: <5°, 5°–10°, 10°–15°, 15°–20°, 20°–25°, 25°–30°, 30°–35°, and >35°. The Fishnet tool in ArcGIS 10.2 was used to extract the raster data to points. The sampling interval was set to 500 m. A total of 19,686 points were extracted and used as the operating data for the geodetector. For areas of different geomorphological types, a uniform method was used to stratify the factors affecting soil erosion to ensure that their effects on erosion were examined under the same spatial stratification conditions, thereby ensuring the comparability of results for areas of different geomorphological types.

## 3 Results and analysis

### 3.1 Statistics of soil erosion and geographic environmental factors for various geomorphological types

In 2010, the soil erosion rates in the Sancha River Basin ranged from 0 to 124.44 t $ha^{-1}a^{-1}$, with an average of 11.37 t $ha^{-1}a^{-1}$. These rates were in relatively good agreement with those in karst peak cluster-depression areas in Guangxi determined by Feng *et al*. (2016) using the $^{137}Cs$ method. In addition, Zeng *et al*. (2017) simulated soil erosion in Yinjiang County, Guizhou Province, using the RUSLE model and reported a soil erosion rate in 2013 of 18.84 t $ha^{-1}a^{-1}$. Febles-Gonzalez *et al*. (2012) simulated soil erosion in the karst regions of Havana, Cuba, and reported erosion rates of 12.3 to 13.7 t $ha^{-1}a^{-1}$, which were relatively close to the soil erosion simulation results obtained in this study. Soil erosion in the Sancha River Basin displayed spatial heterogeneity (Figure 3) and was more severe in the upper and middle reaches than the lower reaches. As shown in Table 3, the geographic environmental factors in various geomorphology distribution areas were also spatially heterogeneous. Mountainous and hilly areas had a relatively high average slope gradient, whereas plain and terrace areas had a relatively low slope gradient. The average elevation of middle relief mountainous areas was significantly higher than that of other areas, whereas the opposite relationship was observed for precipitation. Farmland was mainly concentrated in small- and middle-relief mountainous areas and middle elevation hilly areas. Slope farmland was mainly distributed in small- and middle-relief mountainous and middle elevation hilly areas. The average amount of soil

erosion varied significantly between areas of different geomorphological types. Due to the influence of slope gradients, precipitation and human activities, middle elevation hill had the highest average soil erosion rate, followed by small relief mountainous and middle elevation terrace had the lowest soil erosion rate.

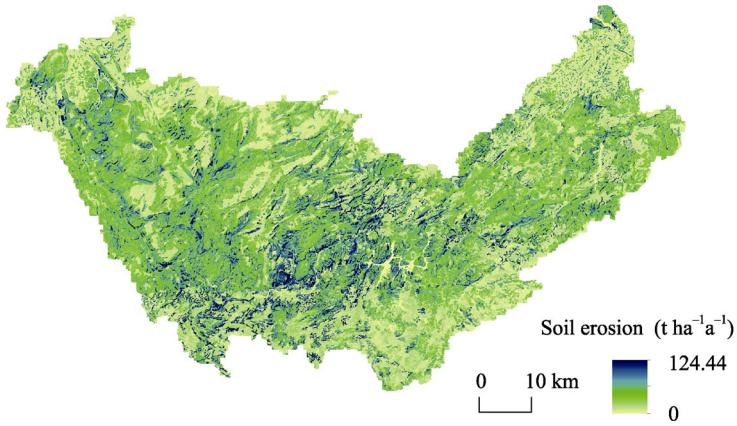


**Figure 3** The spatial distribution of soil erosion in the Sancha River Basin in 2010

**Table 3** Soil erosion and geographic environmental factors in different geomorphological types

| | Soil erosion (t ha$^{-1}$ a$^{-1}$) | Slope (°) | Rainfall (mm) | Elevation (m) | Area of dry land (km$^2$) | Area of steep slopes (km$^2$) | Total area (km$^2$) |
|---|---|---|---|---|---|---|---|
| Middle elevation plain | 8.32 | 4.80 | 1233.82 | 1256.51 | 17.54 | 0.06 | 98.30 |
| Middle elevation terrace | 6.49 | 3.97 | 1172.98 | 1445.74 | 19.92 | 0.02 | 99.64 |
| Middle elevation hill | 12.62 | 11.00 | 1199.28 | 1383.46 | 159.60 | 3.41 | 717.72 |
| Small relief mountain | 11.87 | 14.91 | 1136.88 | 1482.15 | 656.15 | 51.67 | 3016.14 |
| Middle relief mountain | 10.22 | 16.34 | 1096.33 | 1775.38 | 189.62 | 23.70 | 928.89 |

## 3.2 Geodetector-based quantitative attribution analysis of soil erosion in different geomorphological types

### 3.2.1 Significance analysis of factors affecting soil erosion

The results of the factor detector show that the dominant factor affecting soil erosion and its power of determinant varied significantly between areas of different geomorphological types (Table 4). The significance of the effects of influencing factors was affected by the internal characteristics of different geomorphological types. For example, elevation had an insignificant explanatory power for soil erosion in middle elevation terrace but had an explanatory power regarding soil erosion as high as 19.3% in middle relief mountain. Land use type had a significantly higher explanatory power for the spatial distribution of soil erosion (over 51% in areas of various geomorphological types and as high as 68.5% in middle elevation terrace areas) than other influencing factors. The following patterns were observed for the explanatory power of slope for soil erosion. The explanatory power of slope gradient for soil erosion decreased as the relief increased in mountainous and hilly areas, whereas an opposite

pattern was observed for relatively flat areas. Specifically, for mountainous and hilly areas, the value of the *q*-statistic for middle elevation hilly areas was the highest, followed by that for small relief mountainous areas and that for middle relief mountainous areas; for relatively flat areas (plain and terrace areas), the value of the *q*-statistic for middle elevation terrace areas was higher than that for middle elevation plain areas. The explanatory power of precipitation for soil erosion differed considerably between areas of different geomorphological types. The ecological detector shows that the effects of land use on the spatial distribution of soil erosion in middle elevation plain and terrace areas differed significantly from those of other factors. The effects of land use and slope gradient on soil erosion in middle elevation hilly areas and small relief mountainous areas differed significantly from those of other factors. The effects of land use and elevation on soil erosion in middle relief mountainous areas differed considerably from those of other factors.

**Table 4** The *q* values of influencing factors in different geomorphological types

| | Land use | Slope | Rainfall | Lithology | VC | Elevation |
|---|---|---|---|---|---|---|
| Middle elevation plain | 0.622 | 0.082 | 0.091 | – | – | 0.028 |
| Middle elevation terrace | 0.685 | 0.086 | 0.037 | – | – | – |
| Middle elevation hill | 0.513 | 0.126 | 0.010 | 0.031 | 0.059 | 0.010 |
| Small relief mountain | 0.567 | 0.071 | 0.051 | 0.01 | 0.005 | 0.013 |
| Middle relief mountain | 0.620 | 0.062 | 0.089 | 0.037 | 0.005 | 0.193 |

Note: "–" means the *q* value did not pass the significance test; "VC" means vegetation coverage.

### 3.2.2 Analysis of interactions between factors affecting soil erosion

The interaction detector results show that the interaction between any two influencing factors enhanced their explanatory powers of soil erosion in the five geomorphological types. The dominant interaction differed between areas of different geomorphological types. Table 5 summarized the interactions with the three highest explanatory powers. The interaction between land use type and slope gradient has the highest explanatory power (>70%) and is a significant factor controlling soil erosion in areas of all the geomorphological types, except for middle elevation plain areas. This means that soil erosion varied significantly between areas of the same land use type but different slope gradients or areas of the same slope gradient but different land use types. For example, the soil erosion rate differed significantly between a 25° slope farmland area and a 5° slope farmland area or between a 25° slope farmland area and a 25° slope forestland area. Due to relatively low intensity slope cultivation and reasonable land-use patterns (Table 3), the explanatory power of the combination of land use type and slope gradient for soil erosion in middle elevation plain areas was slightly lower but was still as high as 67.1%. In comparison, the combination of land use type and precipitation can explain 71% of the spatial distribution of soil erosion in middle elevation plain areas. The interactions involving the second and third highest explanatory powers for soil erosion in areas of different geomorphological types were those between land use type and other influencing factors, but these interactions varied between areas of different geomorphological types (Table 5). Moreover, the combination of slope gradient and precipitation can significantly nonlinearly increase the explanatory power of each single factor. The explanatory power of the combination of slope gradient and precipitation ranged from

13.8% to 21.3% in the five geomorphological types.

**Table 5** The dominant interactions between two covariates in different geomorphological types

| Geomorphology | Middle elevation plain | Middle elevation terrace | Middle elevation hill | Small relief mountain | Middle relief mountain |
|---|---|---|---|---|---|
| Interaction 1 | Land use∩rainfall | Land use∩slope | Land use∩slope | Land use∩slope | Land use∩slope |
| *q* | 0.710 | 0.764 | 0.726 | 0.707 | 0.742 |
| Interaction 2 | Land use∩VC | Land use∩VC | Land use∩ elevation | Land use∩ rainfall | Land use∩ rainfall |
| *q* | 0.695 | 0.720 | 0.567 | 0.648 | 0.679 |
| Interaction 3 | Land use∩ lithology | Land use∩ rainfall | Landuse∩ rainfall | Land use∩ lithology | Land use∩elevation |
| *q* | 0.682 | 0.708 | 0.566 | 0.586 | 0.665 |

"VC" means vegetation coverage.

**3.2.3** Identification of areas at high risk of soil erosion and determination of the difference in soil erosion between strata of each influencing factor

The factor and interaction detectors show that influencing factors and their combinations had different explanatory powers regarding the spatial distribution of soil erosion. By running the risk detector module, the spatial distribution of soil erosion can be detected, areas at high risk of soil erosion (confidence level: 95%) (Table 6) can be identified, and whether the difference in soil erosion rate between strata of each influencing factor is significant can be determined. On this basis, the percentage of the number of stratified combinations that differed significantly can be determined (Table 7). Areas at high risk of soil erosion varied significantly between areas of different geomorphological types (Table 6). In small relief mountainous areas, the soil erosion rate increased as the slope gradient increased. In areas of the other four geomorphological types, there was an inflection point in the relationship between slope gradient and soil erosion rate (i.e., the high-risk slope areas shown in Table 6). Dry land suffered from the most severe soil erosion; however, the average soil erosion rate varied between different geomorphological types. The variation in the soil erosion rate in the Sancha River Basin as a function of vegetation coverage differed from that in other regions, and there was a critical value of vegetation coverage. When the vegetation coverage was lower than this critical value, the soil erosion rate increased as the vegetation coverage increased; when the vegetation coverage was higher than this critical value, the soil erosion rate decreased as the vegetation coverage increased. Geologic conditions provided the background conditions for soil erosion to occur. Soil erosion rates of different lithological types are related to the climate, terrain and anthropogenic factors. The lithology with most serious soil erosion varied between different geomorphological types. There was no significant positive or negative correlation between elevation and the spatial distribution of soil erosion. In addition, the elevation ranged in which the highest soil erosion rate occurred also varied. The percentage of the number of combinations with significant differences in soil erosion rates between strata of each influencing factor varied considerably between different geomorphological types (Table 7). The difference between strata of land use was the largest (significant difference accounted for over 90%) between areas of different geomorphological types. The difference between strata of slope gradient in areas with a relatively high average

slope gradient (e.g., small- and middle-relief mountainous areas and middle elevation hilly areas) was larger than that in areas with a relatively low average slope gradient (e.g., middle elevation plain and terrace areas). The difference between strata of precipitation and elevation reached 100% in middle elevation plain areas and was larger in small- and middle-relief mountainous areas than middle elevation hilly and terrace areas. The difference between strata of lithology and vegetation coverage was relatively low.

**Table 6** High risk areas of soil erosion and its mean value (t $ha^{-1}$ $a^{-1}$) in different geomorphological types

| | Middle elevation plain | Middle elevation terrace | Middle elevation hill | Small relief mountain | Middle relief mountain |
|---|---|---|---|---|---|
| Slope (°) | 20–25 | 15–20 | 30–35 | >35 | 25–30 |
| Mean value | 19.9 | 19.02 | 24.38 | 22.28 | 14.41 |
| Land use | Dry land | Dry land | Dry land | Dry land | Dry land |
| Mean value | 22.6 | 15.36 | 23.43 | 24.36 | 21.9 |
| VC | 0.5–0.6 | <0.3 | 0.8–0.9 | 0.9–1 | 0.5–0.6 |
| Mean value | 9.35 | 10.02 | 14.5 | 14.17 | 10.7 |
| Lithology | Interbedded limestone and clastic rocks | Limestone with clastic rocks | Clastic rocks | Dolomite with clastic rocks | Dolomite |
| Mean value | 13.93 | 9.49 | 19.52 | 15.59 | 20.07 |
| Elevation (m) | 1087–1235 | 1531–1679 | 1383–1531 | 1383–1531 | 1235–1383 |
| Mean value | 11.1 | 13.13 | 12.15 | 12.44 | 15.84 |

"VC" means vegetation coverage

**Table 7** The percentage of stratification combinations with significant difference in each influencing factor (%)

| | Middle elevation plain | Middle elevation terrace | Middle elevation hill | Small relief mountain | Middle relief mountain |
|---|---|---|---|---|---|
| Land use | 90.91 | 100.00 | 92.86 | 100.00 | 93.33 |
| Slope | 40.00 | 16.67 | 78.57 | 92.86 | 85.71 |
| Rainfall | 100.00 | 33.33 | 33.33 | 91.67 | 78.57 |
| Elevation | 100.00 | 0.00 | 42.86 | 69.44 | 75.00 |
| Lithology | 0.00 | 0.00 | 60.00 | 64.44 | 55.56 |
| VC | 33.33 | 35.71 | 75.00 | 60.71 | 60.71 |

"VC" means vegetation coverage

## 4 Discussion

The geomorphological types macroscopically control the occurrence and development of surface processes. As a type of surface process, soil erosion displays significantly different characteristics in different geomorphological types. Land use type was the most significant factor. The explanatory power of the slope gradient regarding soil erosion was significantly higher in relatively flat areas (e.g., middle elevation plain, hilly and terrace areas) than in areas of higher relief (e.g., small- and middle-relief mountainous areas). This pattern caused by that relatively steep areas have complex terrain and large climate variations and are ecologically vulnerable, and factors affecting soil erosion in these areas are more complex. Consequently, the slope gradient had a lower spatial explanatory power regarding soil ero-

sion in these areas. Compared to the other four geomorphological types, elevation has the highest explanatory power regarding soil erosion in middle relief mountainous areas. This pattern existed because middle relief mountainous areas were characterized by large internal height differences and notable vertical variations of vegetation, and consequently, elevation stratification can reflect the comprehensive difference in vegetation, climate and terrain. The effects of lithology and vegetation coverage on soil erosion were insignificant in middle elevation plain and terrace areas. Although these factors significantly affected the occurrence of soil erosion on a slope scale, their controlling effects on soil erosion in areas of specific geomorphological types were insignificant.

Due to the complexity of geographic processes, controlling factors often do not act independently but instead act collectively. The extent to which the effects of controlling factors combined remains an unresolved issue. This study examined the interaction between any two of the factors affecting soil erosion using the geodetector method to determine its pattern. The results show that the interaction between slope gradient and land use type had an explanatory power regarding soil erosion as high as over 67% in areas of each geomorphological type. Wang *et al*. (2013) once noted that the effects of various land use types on soil erosion in the Wujiang River Basin differed significantly and the soil erosion rate increased significantly as the slope gradient increased. This finding agreed with the finding of this study: the interaction between slope gradient and land use type can significantly enhance their controlling effects on soil erosion. The results also demonstrated the necessity of returning farmland to forestland and prohibiting steep slope land farming. In addition, the combination of slope gradient and precipitation enhanced their explanatory powers regarding soil erosion. Slope gradient and precipitation are the necessary conditions and dynamic basis for soil erosion to occur. When falling on steep slopes, precipitation can easily lead to water erosion. The combination of slope gradient and lithology can also enhance their explanatory powers regarding soil erosion. Rock is the basic material of soil. Different lithologic backgrounds determined the characteristics of subsurface rock layers and topsoil. In a karst region, rocks were very slowly transformed to soil by weathering, soils were shallow and lacked a layer of parent material, and there was a notable soft/hard interface between soil masses and rocks (Cai *et al*., 2015). Thus, areas with a relatively high slope gradient were extremely prone to soil erosion due to gravity or other external forces.

Chen *et al*. (2014) noted that soil erosion rates in soil-rock hilly areas in southern China first increased and then decreased as the slope gradient increased and that the critical slope gradient at the inflection point was 15°–25°. A similar conclusion is derived from this study. The critical slope gradient was 20°–25° in middle elevation plain areas, 30°–35° in middle elevation hilly areas, 15°–20° in middle elevation terrace areas and 25°–30° in middle relief mountainous areas. Earlier work has indicated that the effects of vegetation coverage on soil erosion in the Wujiang River Basin involved a critical value (Wang *et al*., 2013). The results obtained in this study show that the critical vegetation coverage in middle relief mountainous and middle elevation plain areas was 0.5–0.6, caused by that areas with dense vegetation coverage often have a high slope gradient. In addition, the precipitation, lithology and slope gradient in areas at high risk of soil erosion varied significantly between areas of different geomorphological types. The difference in soil erosion rates between strata of each influencing factor varied significantly between areas of different geomorphological types. The

difference between strata of land use type was the largest. The difference between strata of each of the other factors (e.g., slope gradient, precipitation, elevation, lithology, and vegetation coverage) varied. Therefore, it is necessary to formulate policies and select key soil erosion control areas based on local conditions and comprehensive consideration of the spatial distribution of soil erosion and the difference between strata of each influencing factor in areas of different geomorphological types.

Researchers in China and elsewhere have studied soil erosion on various scales using various methods. The poor comparability of their results was unfavorable for result validation. Of the numerous methods, the capability of the RUSLE model, the most popular empirical equation used in China and elsewhere, for large-scale erosion simulation has been generally recognized. In this study, considering factors (e.g., outcropping bedrocks and effective slope length) unique to karst regions, a 9-m DEM was selected for the RUSLE model, which significantly improved the simulation accuracy of the *LS* factor. However, there are still some limitations. The soil layers in some areas of the karst region are shallow. In areas that have suffered from severe rocky desertification, there is less erodible soil. The RUSLE model, to some extent, overestimated soil erosion in the Sancha River Basin. The RUSLE model correction based on soil thickness will be a focus of future research.

## 5 Conclusions

This study analyzed the dominant factors affecting the spatial distribution of soil erosion in areas of various geomorphological types and the degree of interaction between any two of these factors using the geodetector method, and identified areas at high risk of soil erosion and the difference in soil erosion rates between strata of each factor. The following conclusions were derived from the findings and can be used as a reference for soil erosion control.

(1) The six influencing factors selected in this study have different explanatory powers regarding soil erosion. Land use type has the highest explanatory power in areas of the five geomorphological types. The effects of influencing factors and their interactions on soil erosion varied between different geomorphological types.

(2) The interaction effect between two influencing factors can enhance their explanatory powers regarding soil erosion. The combination of land use type and slope gradient was most significant. Measures such as prohibiting slope farming and returning farmland to forestland can effectively prevent local soil erosion. The combination of slope gradient and precipitation significantly improved their explanatory powers regarding soil erosion. Therefore, necessary prevention and control measures should be implemented in steep areas where heavy precipitation may occur to reduce economic losses caused by disasters.

(3) To control soil erosion, it is necessary to comprehensively consider the macroscopic controlling effects of geomorphological types. According to the results of quantitative attribution analysis in this study, key soil erosion control areas were determined in areas of different geomorphological types. The followings were the key soil erosion control areas in small relief mountainous areas: steep slopes with a gradient steeper than 35°, areas between elevations of 1383 and 1531 m, dry land, and areas where dolomite with clastic rocks distributed. In middle relief mountainous areas: slopes with a gradient of 25°–30°, areas between elevations of 1235 and 1383 m, dry land, and areas where dolomite is distributed. In middle elevation plain areas: slopes with a gradient of 20°–25°, areas between elevations of

1087 m and 1235 m, dry land, and areas where interbedded limestone and clastic rocks are distributed. In middle elevation hilly areas: slopes with a gradient of 30°–35°, areas between elevations of 1383 and 1531 m, dry land, and areas where clastic rocks are distributed. In middle elevation terrace areas: slopes with a gradient of 15°–20°, areas between elevations of 1531 and 1679 m, dry land, and areas where limestone with clastic rocks is distributed.

## References

Arnoldus H M J, 1980. An approximation of the rainfall factor in the universal soil loss equation. In: De Boodt M, Gabriels D. Assessment of Erosion. Chichester UK: Wiley, 127–132.

Bai X, Zhang X, Long Y *et al*., 2013. Use of $^{137}Cs$ and $^{210}Pb_{ex}$ measurements on deposits in a karst depression to study the erosional response of a small karst catchment in southwest China to land-use change. *Hydrological Processes*, 27(6): 822–829.

Cai Y, Wan J, Wang Y *et al*., 2015. Study on Land Change in Guizhou Karst Plateau Mountain Area. Beijing: Science Press, 61–62. (in Chinese)

Chen S, Yang X, Xiao L *et al*., 2014. Study of soil erosion in the southern hillside area of China based on RUSLE model. *Resources Science*, 36(6): 1288–1297. (in Chinese)

Dai Q, Peng X, Wang P *et al*., 2018. Surface erosion and underground leakage of yellow soil on slopes in karst regions of southwest China. *Land Degradation & Development*, 29(8): 2438–2448.

Febles-Gonzalez J M, Vega-Carreno M B, Tolon-Becerra A *et al*., 2012. Assessment of soil erosion in karst regions of Havana, Cuba. *Land Degradation & Development*, 23(5): 465–474.

Feng T, Chen H, Polyakov V O *et al*., 2016. Soil erosion rates in two karst peak-cluster depression basins of northwest Guangxi, China: Comparison of the RUSLE model with $^{137}Cs$ measurements. *Geomorphology*, 253: 217–224.

Gutierrez F, Parise M, De Waele J *et al*., 2014. A review on natural and human-induced geohazards and impacts in karst. *Earth-Science Reviews*, 138: 61–88.

Hou W, Gao J, Peng T *et al*., 2016. Review of ecosystem vulnerability studies in the karst region of southwest China based on a structure-function-habitat framework. *Progress in Geography*, 35(3): 320–330. (in Chinese)

Hu Y, Wang J, Li X *et al*., 2011. Geographical detector-based risk assessment of the under-five mortality in the 2008 Wenchuan earthquake, China. *Plos One*, 6(6): e21427.

Hutchinson M F, 2002. Anusplin Version 4.2 User Guide. Centre for resource and environment studies. Canberra: Austrilian National University.

Li J, Lu D, Xu C *et al*., 2017. Spatial heterogeneity and its changes of population on the two sides of Hu Line. *Acta Geographica Sinica*, 72(1): 148–160. (in Chinese)

Li Z, Cao W, Liu B *et al*., 2008. Current status and developing trend of soil erosion in China. *Science of Soil & Water Conservation*, 6(1): 57–62. (in Chinese)

Luo W, Jasiewicz J, Stepinski T *et al*., 2016. Spatial association between dissection density and environmental factors over the entire conterminous United States. *Geophysical Research Letters*, 43(2): 692–700.

McCool D K, Brown L C, Foster G R *et al*., 1987. Revised slope steepness factor for the universal soil loss equation.*Transactions of the Asae*, 30(5): 1387–1396.

McCool D K, Foster G R, Mutchler C K *et al*., 1989. Revised slope length factor for the universal soil loss equation. *Transactions of the ASAE*, 32(5): 1571–1576.

Peng T, Wang S, 2012. Effects of land use, land cover and rainfall regimes on the surface runoff and soil loss on karst slopes in southwest China. *Catena*, 90(1): 53–62.

Peng X, Dai Q, Li C *et al*., 2018. Role of underground fissure flow in near-surface rainfall-runoff process on a rock mantled slope in the karst rocky desertification area. *Engineering Geology*, 243: 10–17.

Renard K G, Foster G R, Weesies G A *et al*., 1997. Predicting soil erosion by water: A guide to conservation planning with the revised universal soil loss equation (RUSLE). Agriculture handbook. USDA, Washington, DC.

Tong L, Xu X, Fu Y *et al*., 2014. Impact of environmental factors on snail distribution using geographical detector model. *Progress in Geography*, 33(5): 625–635. (in Chinese)

Wang J, Li X, Christakos G *et al*., 2010. Geographical detectors-based health risk assessment and its application in the neural tube defects study of the Heshun region, China. *International Journal of Geographical Information Science*, 24(1): 107–127.

Wang J, Xu C, 2017. Geodetector: Principle and prospective. *Acta Geographica Sinica*, 72(1): 116–134. (in Chinese)

Wang S, Liu Q, Zhang D, 2004. Karst rocky desertification in southwestern China: Geomorphology, landuse, impact and rehabilitation. *Land Degradation & Development*, 15(2): 115–121.

Wang Y, Cai Y, Pan M, 2013. Analysis on the relationship between soil erosion and land use in Wujiang River Basin in Guizhou province. *Research of Soil and Water Conservation*, 20(3): 11–18. (in Chinese)

Williams J, Jones C A, Kiniry J R *et al*., 1989. The EPIC crop growth-model. T*ransactions of the ASAE*, 32(2): 497–511.

Xiong K, Li J, Long M, 2012. Features of soil and water loss and key issues in demonstration areas for combating karst rocky desertification. *Acta Geographica Sinica*, 67(7): 878–888. (in Chinese)

Xu Y, Shao X, 2006. Estimation of soil erosion supported by GIS and RUSLE: A case study of Maotiaohe watershed, Guizhou province. *Journal of Beijing Forestry University*, 28(4): 67–71. (in Chinese)

Yan Y, Dai Q, Yuan Y *et al*., 2018. Effects of rainfall intensity on runoff and sediment yields on bare slopes in a karst area, SW China. *Geoderma*, 330: 30–40.

Zeng C, Wang S, Bai X *et al*., 2017. Soil erosion evolution and spatial correlation analysis in a typical karst geomorphology using RUSLE with GIS. *Solid Earth*, 8(4): 1–26.

Zhan D, Zhang W, Yu J *et al*., 2015. Analysis of influencing mechanism of residents' livability satisfaction in Beijing using geographical detector. *Progress in Geography*, 34(8): 966–975. (in Chinese)

Zhang H, Yang Q, Li R *et al*., 2013a. Extension of a GIS procedure for calculating the RUSLE equation *LS* factor. *Computers & Geosciences*, 52: 177–188.

Zhang X, Wang S, Bai X *et al*., 2013b. Relationships between the spatial distribution of karst land desertification and geomorphology, lithology, precipitation, and population density in Guizhou province. *Earth & Environment*, 41(1): 1–6. (in Chinese)

Zhang X, Wang S, He X *et al*., 2007. Soil creeping in weathering crusts of carbonate rocks and underground soil losses on karst slopes. *Earth & Environment*, 35(3): 202–206. (in Chinese)

Zhou C, Cheng W, Qian J *et al*., 2009. Research on the classification system of digital land geomorphology of 1:1000000 in China. *Journal of Geo-information Science*, 11(6): 707–724. (in Chinese)